IN-SITU TEM OBSERVATION OF Pd CATALYZED GRAPHENE GROWTH BY **CURRENT-INDUCED ANNEALING**

Mohamad Saufi Rosmi^{1,2,*}, Yazid Yaakob³, Mohamad Azuwa Mohamed², Siti Munirah Sidik¹ and Tanemura Masaki⁴

¹Department of Chemistry, Faculty of Science and Mathematics, Universiti Pendidikan Sultan Idris, 35900 Tanjong Malim, Perak, Malaysia

²Department of Chemical Sciences, Faculty of Science and Technology, Universiti Kebangsaan Malaysia, 43600 UKM Bangi, Selangor, Malaysia

³Department of Physics, Faculty of Science, Universiti Putra Malaysia, 43400 UPM Serdang, Selangor, Malaysia

⁴Department of Physical Science and Engineering, Graduate School of Engineering, Nagoya Institute of Technology, Gokiso-cho, Showaku, Nagoya 466-8555, Japan

*saufirosmi@fsmt.upsi.edu.my

Abstract. The use of Palladium (Pd) as a substrate for studying graphene growth presents a unique avenue of exploration. Pd is known as a "carbon sponge" with extensively studied carbon solubility and diffusivity. This study uses Pd as a catalyst for studying graphene growth, revealing a solid-phase reaction process in *in-situ* transmission electron microscopy (TEM). The study reveals significant structural changes in amorphous carbon nanofibers (CNF) catalyzed with Pd when electrical potential is applied through two- probe system. Notably, the gradual recrystallization and agglomeration of Pd particles, beginning in the middle segment of the CNF and advancing toward the end, were observed under high current flow ranging from 0.35 µA to 12 µA. This transformation, influenced by joule heating and significant thermal gradients, led to the crystallization of amorphous carbon, resulting in sp² hybridized carbon formation and the formation of graphene sheets starting from the Pd surface's tip. Structural deformation and the breaking of the graphene sheet were observed at higher current flow of 35.0 µA due to saturated current flow and induced Joule heating. The successful synthesis of graphene with approximately 350 nm between the cathode and anode, was achieved within the *in-situ* TEM environment. This *in-situ* TEM approach provides insights into carbon-Pd interactions and addresses a significant research gap by enabling the observation of graphene formation at the nanoscale.

Keywords: Graphene, palladium, solid phase reaction, *in-situ* TEM

Article Info

Received 20th September 2023 Accepted 17th May 2024

Published 12th June 2024

Copyright Malaysian Journal of Microscopy (2024). All rights reserved.

ISSN: 1823-7010, eISSN: 2600-7444

1. INTRODUCTION

Graphene, a remarkable two-dimensional material composed of sp² hybridized carbon atoms arranged in a honeycomb structure, has been successfully synthesized on metal catalysts such as Ni and Pt, using various hydrocarbon sources as precursors [1]. However, despite extensive research on these metal catalysts, there has been limited exploration of graphene synthesis on Pd catalysts, which belong to the same group as Ni and Pt in the periodic table [2]. The intriguing aspect of Pd as a catalyst lies in its unique equilibrium of C-Pd distance and binding energy per atom, differing from the C-Pt and C-Ni systems [3]. This distinct characteristic places Pd in a potentially unique position within the elemental group, offering a novel avenue for graphene synthesis [4]. Furthermore, from an application standpoint, graphene growth on Pd substrates exhibits semiconductor-like properties, featuring a band gap of approximately 0.3 eV [5]. Despite significant progress in understanding the synthesis of graphene on Pd substrates, the precise mechanism behind its growth remains enigmatic.

Transmission electron microscopy (TEM) has emerged as an indispensable tool for comprehending carbon deposition on 3d transition metals like Ni, Fe, Cu, and Pt catalysts [6]. It has provided valuable insights into the underlying processes. In our earlier study, we used in situ transmission electron microscopy (TEM) to illustrate the graphitization process in solid phase reaction for metal nanoparticles and amorphous carbon nanofibers (CNFs) [7]. Amorphous carbon transformed into graphene, partially graphitized carbon structure, and multi-wall carbon nanotube (CNT) during electron current flow for Cu-coated CNFs, Agincorporated CNFs, and Fe-incorporated CNFs, respectively, during the migration or evaporation of metal nanoparticles, depending on the catalytic activity of the metal.

Despite these efforts, the precise mechanism governing carbon formation and growth remains a topic of intense debate [8]. In general, hybridized carbon is formed when hydrocarbons adsorb onto metal surfaces before undergoing a series of steps, including gradual dehydrogenation and breaking C–C bonds to form carbon. These nascent carbon atoms then migrate from adsorption sites through one of two pathways to centers for graphene growth [9]. The popular route involves carbon dissolution into metal nanoparticles' bulk. Once saturation occurs, carbon segregates to the metal surface, initiating graphene formation. Various factors significantly influence the process of forming carbon on these metals. These include the metal's capacity for bulk carbon solubility, the movement of carbon atoms within the metal structure, which can be deduced from alterations in lattice parameters, the formation of carbides at elevated temperatures, and insights gained from kinetic studies [10].

Expanding on the exploration of solid-phase reactions between metals and amorphous carbon, our focus now turns to the metal palladium (Pd). Previous research has reported the successful incorporation of Pd into carbon nanofibers (CNF), leading to a significant enhancement in CNF conductivity, particularly in the context of interconnect applications [11]. This improvement is attributed to Pd's ability to enhance contact morphology, ultimately reducing resistance within the CNF structure. While studies have examined contact resistance in CNF structures, particularly in the realm of via technology, there remains a notable research gap concerning the intrinsic properties and structural evolution of nanofibers when subjected to current flow, particularly in integrated circuit applications [12].

Recent investigations into thermal and electrical transports in CNF have revealed a close correlation between breakdown and Joule heating [13-15]. The critical question that arises is the impact of this Joule heating phenomenon on the CNF structure, especially in the presence of metals integrated into CNF. To address this knowledge gap, our study is dedicated to unraveling the fundamental structural evolution of Pd-catalyzed carbon nanofibers (Pd-CNF) under the influence of high current flow using in-situ transmission electron microscopy (TEM) facilities. Here, the dynamic changes occurring within the Pd-CNF structure during these processes were directly observed. This research not only contributes to our understanding of Pd's role as a catalyst but also sheds light on the intricate interplay between current flow and nanofiber morphology, which is crucial for advancing integrated circuit applications.

2. MATERIALS AND METHODS

The Pd-included carbon nanofibers (Pd-CNF) preparation employed commercially available graphite foils with 2.5 x 0.5 x 0.01 cm dimensions. To achieve this goal, a Kaufmann-type ion gun (Iontech, Inc., model 3-1500-100FC) was utilized. A sample stage is affixed to the graphite foil, while a Pd plate, which supplies Pd atoms, is placed perpendicular to the edge of the graphite foil (Figure 1(a)). The graphite and Pd foils were subjected to argon ions (Ar+) at ambient temperature for 60 minutes, with the ions directed at a 45° relative to the surface. The experiment employed a 6 cm diameter and a 1 keV ion beam energy. The working pressure was 2.0 x 10⁻² Pa, while the baseline pressure was 1.5 x 10⁻⁵ Pa. A detailed explanation of the growth mechanism of ion-induced carbon nanofibers has previously been presented [7]. Figure 1(b) provides a scanning electron microscope (SEM) image of the resulting Pd-CNFs after ion irradiation. Subsequently, these Pd-CNFs were affixed to a cathode microprobe within a transmission electron microscope (TEM) (JEM2010, JEOL Co., Japan) operating at 200 kV. A tungsten (W) nanoprobe was used as an anode and mounted on a piezo-driven stage, as depicted in Figure 1(b). During the experiments, TEM images were continuously captured using a CCD camera and dedicated image recording software. The investigation of structural changes in the Pd-CNFs during current-voltage (I-V) measurements was undertaken.

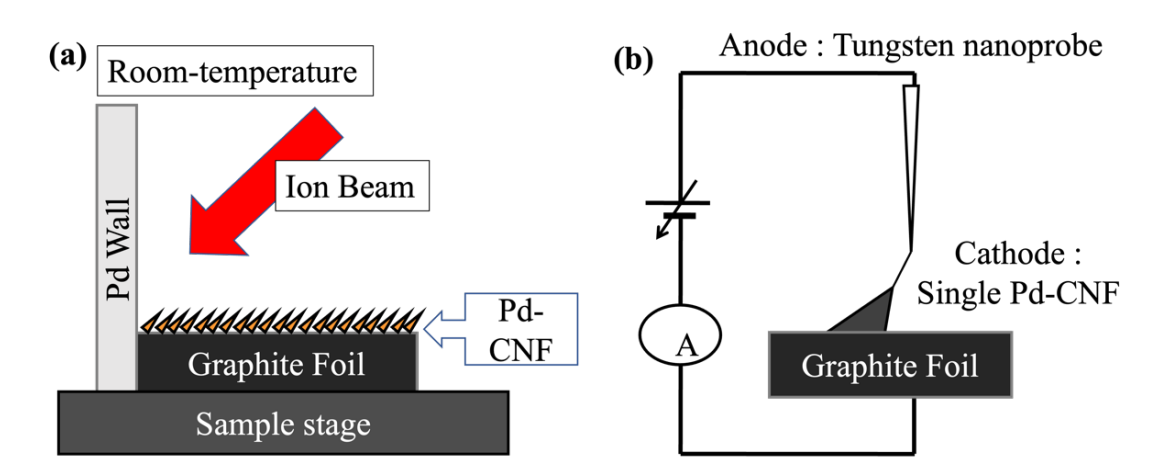


Figure 1: (a) The schematic illustration of the experimental setup for fabrication of Pd-CNFs and (b) Experimental arrangement for in-situ current-voltage (I-V) measurements inside the transmission electron microscope (TEM)

3. RESULTS AND DISCUSSION

In Figure 2(a), low magnification TEM images of Pd-CNFs are presented, showcasing their dimensions at approximately 350 nm in length and about 20 nm diameter. In Figures 2(b) to (d), high magnification TEM images are facilitated for the cone (base), middle, and tip regions of the Pd-CNF, respectively. In these images, the presence of palladium (Pd) is noted in clustered formations, being well-dispersed within the amorphous carbon CNF matrix. Notably, no distinct boundary is discernible between the CNF and the conical tip, and a conspicuous absence of hollow structures is observed, indicative of a fibrous nature rather than a tubular one, thereby distinguishing them from carbon nanotubes (CNTs) or graphene structures.

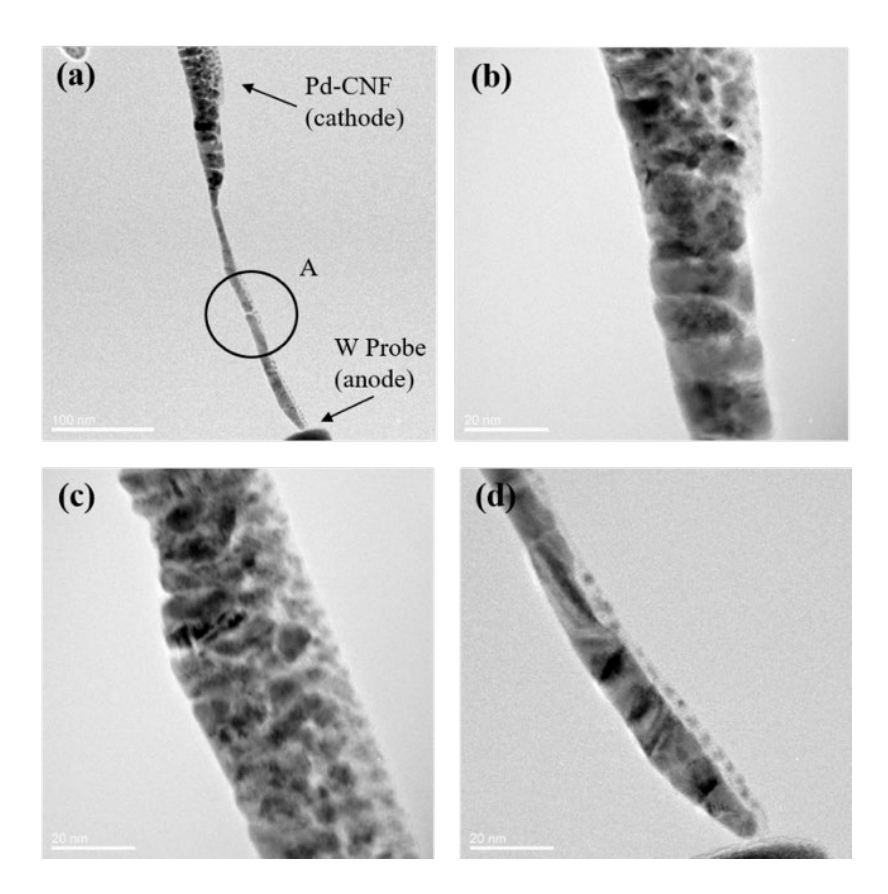
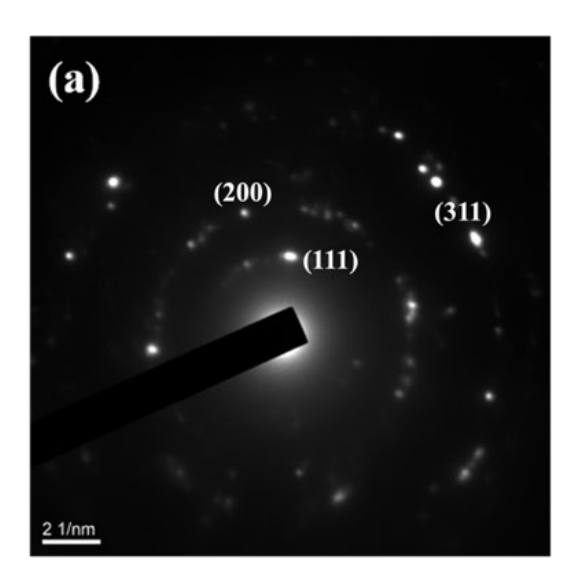


Figure 2: (a) The TEM image of the initial Pd-CNF employed for I-V measurement. High-magnification images were captured for the (b) base, (c) middle, and (d) tip regions of the fiber

In Figure 3(a) and (b), the SAED pattern and EDS results of the region labeled "A" in Figure 2(a) are displayed. The diffraction pattern reveals a polycrystalline ring pattern of Pd and a diffraction ring of amorphous carbon [16], signifying the presence of a blend of amorphous carbon and randomly oriented Pd crystallites within the Pd-CNF, as confirmed by the EDS findings.



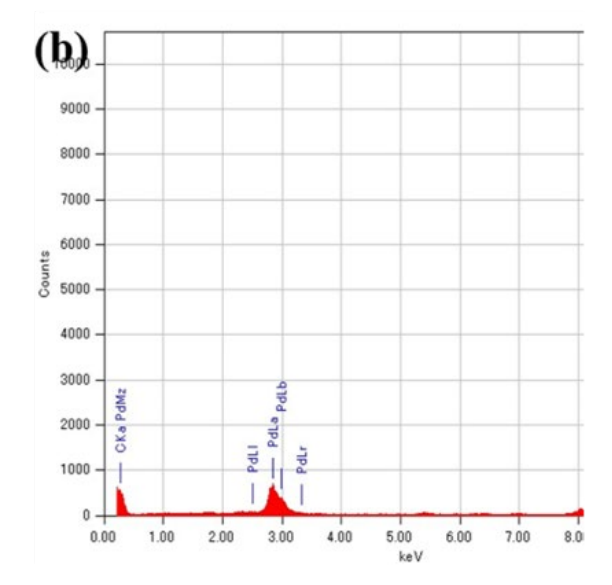


Figure 3: (a) The SAED pattern and (b) EDS spectra of the Pd-CNF obtained from the region of the fiber labeled "A" in Figure 6.2(a)

The investigation of the electrical properties of Pd-CNF involved conducting I-V measurements by applying a bias voltage between the anode W probe and cathode Pd-CNF within the TEM. Incremental steps of 9 mVs⁻¹ were used to apply a low bias voltage, gradually reaching up to 1.0 V, while simultaneously monitoring structural changes in the Pd-CNF.

In Figure 4(a), the I-V characteristic of the Pd-CNF is depicted, revealing a nonlinear increase in current with the rise in bias voltage. Up to 0.65 V, there was no significant augmentation in current flow through the Pd-CNF, only reaching around 0.35 μ A at 173 seconds. However, at 0.70 V, the current gradually escalated until it reached a maximum of 12 μ A. Figure 4(b) illustrates that at 178 seconds, Pd commenced migrating from the middle portion of the CNF towards both the tip and base. This migration was attributed to the Joule heating effect, beginning in the middle, where temperatures were highest due to the high resistance (low diameter)[15]. The migration persisted until the current flow ceased, with Pd particles leaving behind the low crystalline graphene sp² structure during their journey. Figure 5(a) to (d) presents TEM images of the Pd-CNF after a low current flow of 1.0 V. Similar to the TEM image from the video clip in Figure 4(b) (at 219 seconds), displayed in

Figure 5(a), it is found that Pd particles migrated towards both the base and tip sections, leaving behind a low crystalline graphene structure. To further confirm this observation, we captured high-magnification TEM images. In Figure 5(b), a close-up image of the cone section (part A) reveals an accumulation of Pd particles (red arrow). The carbon surrounding the Pd metal appears to be partially graphitized. Figure 5(c) depicts a low crystalline, few-layer graphene sheet in the middle portion of the structure. Notably, the presence of Pd led to the crystallization of the surrounding amorphous carbon, forming sp² carbon bonds. Figure 5(d) showcases the structure's tip part. It's noteworthy that the small Pd nanoparticles existing before the current flow had agglomerated with larger Pd metal islands, leaving behind a low crystalline graphene structure.

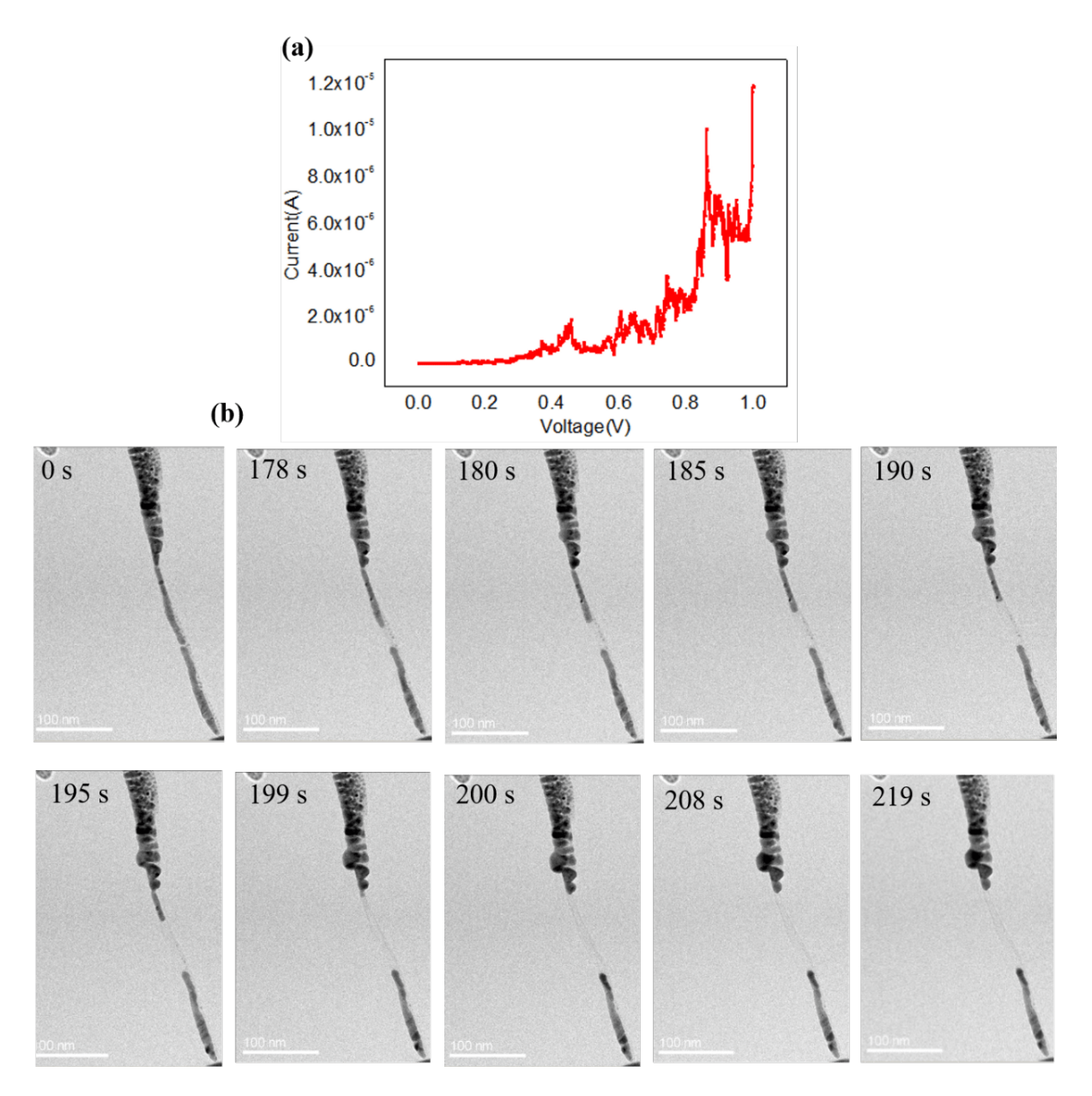


Figure 4: (a) The I-V curve of the Pd-CNF measured using a low bias voltage range of 0–1.0 V in a two-probe system and (b) Video clip of TEM images of the Pd-CNF varies in the applied potential from 0.0–1.0 V to align with the I-V characteristics. These images revealed the gradual structural changes occurring as the applied potential increased (Figure 4 (a))

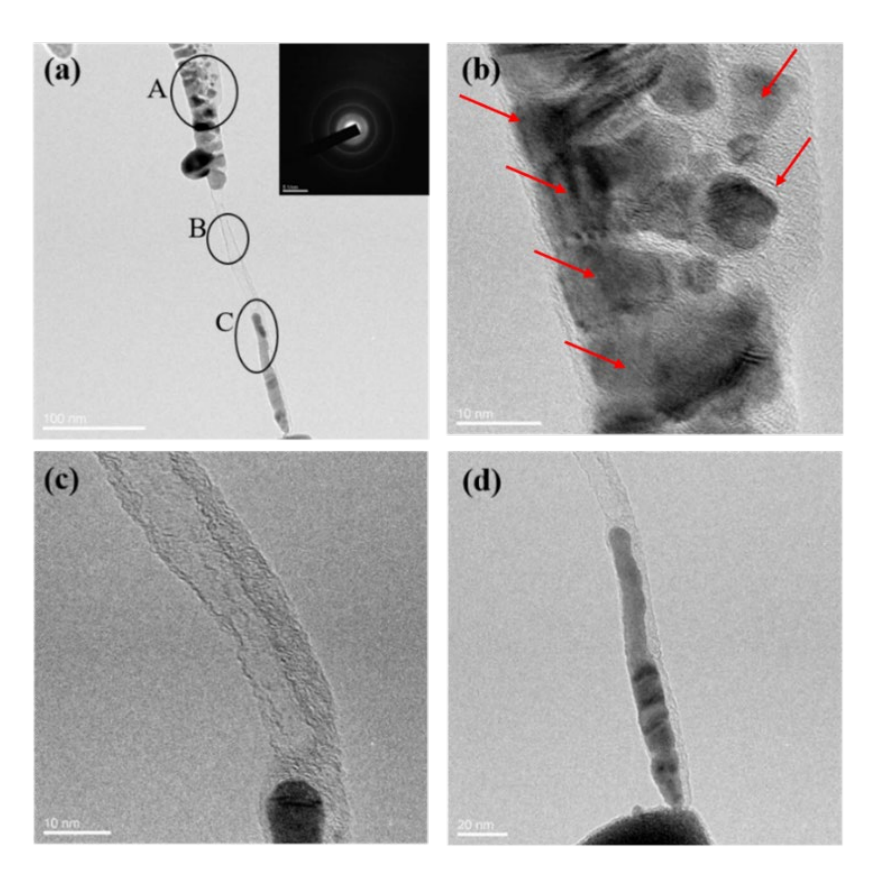


Figure 5: (a) A TEM image of Pd-CNF obtained after applying a low 1.0 V bias voltage, (b) High-magnification TEM images were captured for (c) region A (cone), (d) region B (middle of graphene) and (e) region C (tip of graphene where Pd is still present)

The interesting phenomenon of graphene formation in the presence of Pd was further explored by applying a higher potential of 1.5 V. In Figure 6(a), the I-V characteristic across the Pd-CNF is depicted. It can be observed that the current gradually increases from 0 V to 0.8 V (95 seconds), peaking at a maximum of 2 µA. After reaching 0.8 V, there is a significant surge in current, reaching 16 µA and continuing to rise until it reaches a maximum of 18 µA at 1.5 V. Analyzing a snapshot from the video during the current flow (Figure 6(b)), it is noteworthy that Pd initiates migration towards the base segment at 103 seconds, just a few moments after the notable current surge. The current just before and after this abrupt increase is approximately 2.0 and 18.0 µA, respectively. Consequently, the Joule heat generated after this abrupt current increase is estimated to be about 9 times higher than before, as Joule heat is directly proportional to current × voltage. This suggests that the temperature around the middle area of the structure, following the abrupt current increase, becomes approximately 9 times higher, potentially facilitating the formation of a graphitized structure. Subsequently, at 113 seconds, as one-half of the Pd migrates to the cone section, the other portion of Pd starts moving towards the tip segment. This migration process continues until all the Pd particles have vacated the graphene structure.

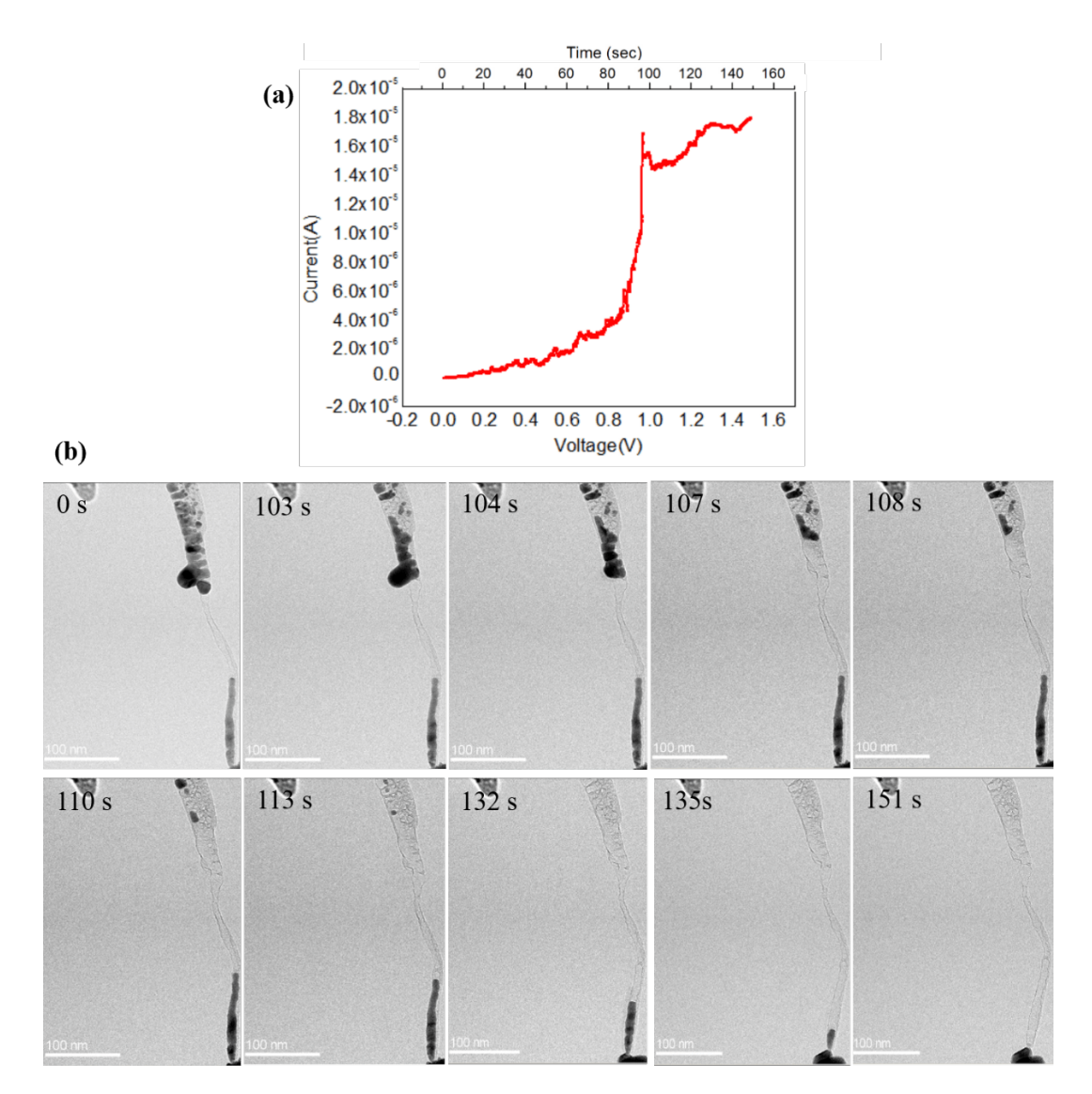


Figure 6: (a) The I-V curve of the Pd-CNF, measured using a high bias voltage range of 0–1.5 V in the two-probe system and (b) A video clip showing TEM images of the Pd-CNF while changing the applied potential from 0.0–1.5 V, corresponding to the I-V characteristics

Figure 7(a) to (d) represents the TEM images of graphene after complete growth facilitated by the Pd catalyst. In Figure 7(a), it is evident that 350 nm of graphene has been successfully synthesized through current-induced annealing. To validate this, high-magnification images were captured to scrutinize the graphene structure. Figure 7(b) provides a close-up of region A, revealing an average of 4 graphene layers. An inter-planar spacing of approximately 0.345 nm is estimated for these graphene layers, consistent with graphite (0002) spacing [17]. Besides that, in Figure 7(c) and (d), high-magnification images from regions B and C unveil the presence of high-quality graphene, further confirming the successful growth process. The size of graphene varies depending on the particle size of Pd, the same phenomenon as reported by Yaakob et al. [14].

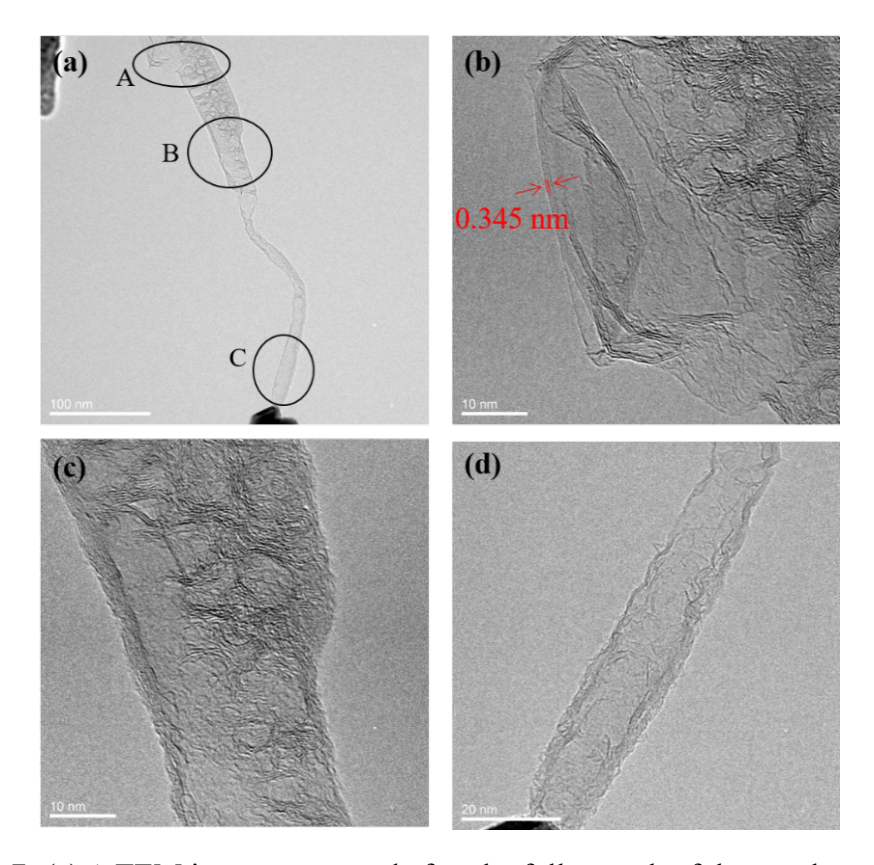


Figure 7: (a) A TEM images captured after the full growth of the graphene. High-magnification TEM images of the graphene in (b) region A, (c) region B, and (d) region C (tip).

After the TEM observation, current properties were compared between Pd-CNF and the resulting graphene (Figure 8(a)). Notably, Pd-CNF exhibited a much lower maximum current flow at a 1 V bias, with values of 0.5 A compared to graphene's 5.0 A. This difference arises from amorphous carbon's high resistance in contrast to the superior conductivity of the sp2 graphitic structure in graphene. The linear I-V curve signifies a strong Ohmic contact between the W electrode and graphene, enabling an electrical current of 5.0 A under a modest 1 V bias voltage.

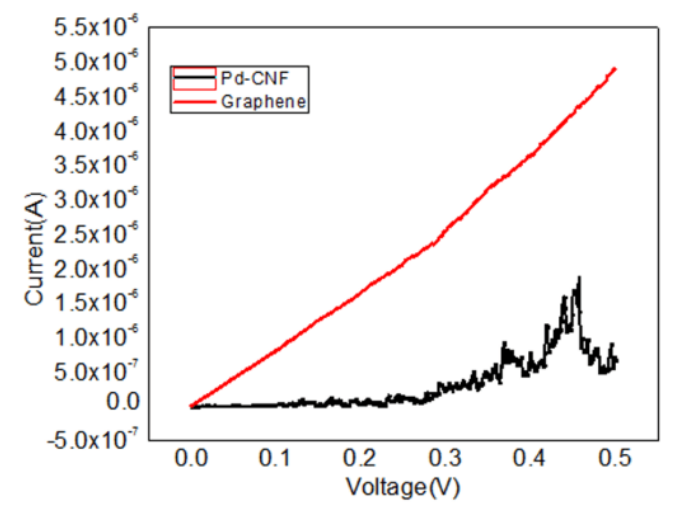


Figure 8: The I-V curve of Pd-CNF and graphene as subjected to an applied voltage of 0.5 V

After the complete growth of graphene, an investigation was conducted to assess the impact of a higher applied potential between the cathode and anode using in-situ TEM. The maximum current flow and electrical breakdown behavior of the graphene were examined by applying a 2.0 V bias voltage. In Figure 9(a), a gradual increase in current was observed until it peaked at 35.0 µA at 1.70 V, subsequently experiencing a sudden and sharp drop to 0 A. Figure 9(b) illustrates that the graphene fractured at its smallest diameter, located at the midpoint. High-magnification images detailing the fractured graphene structure are provided in Figure 9(c) and (d).

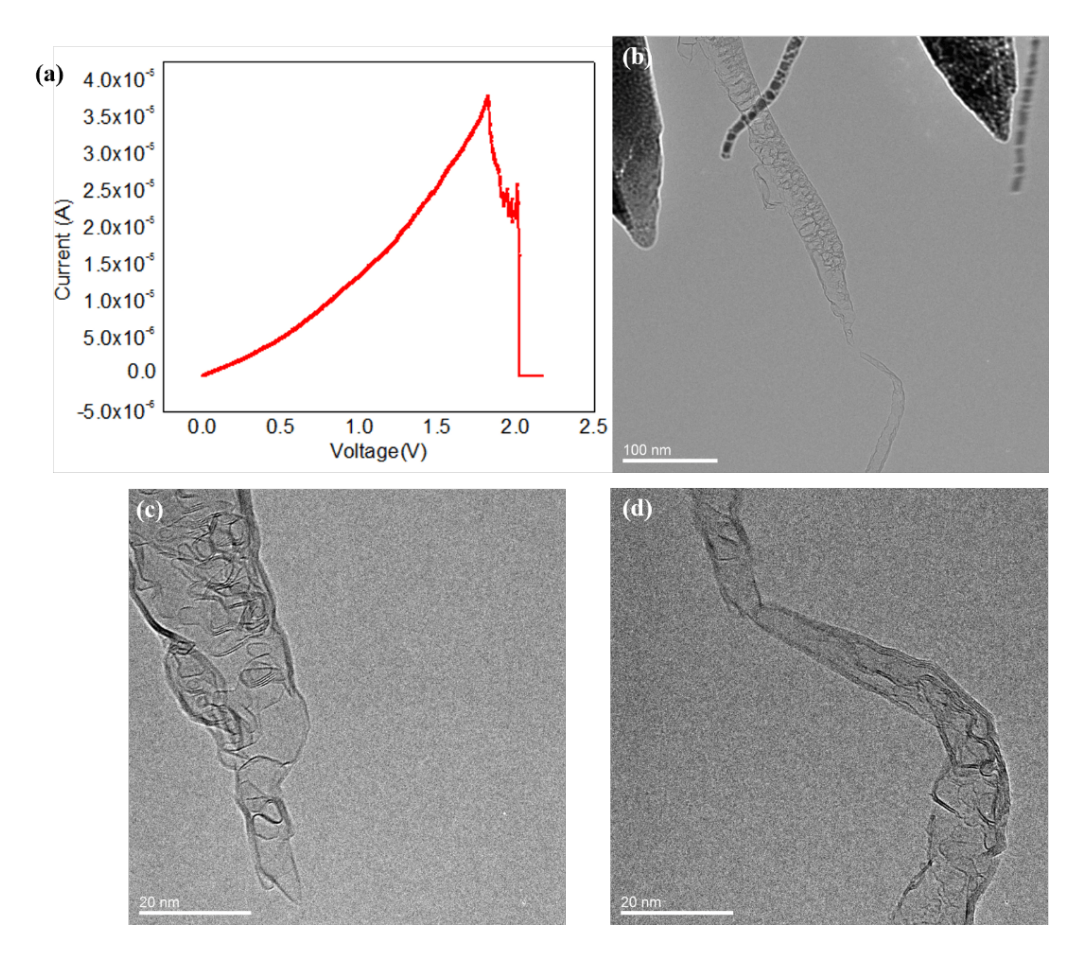


Figure 9: (a) The I-V characteristic under a greater applied potential between the anode and cathode, (b) TEM images of broken CNTs and high-resolution TEM images of the broken and disconnected graphene sheets at (c) the base and (d) the middle parts

The growth model's schematic pictures in Figure 10 are used to explain how the Pd-assisted graphene structure formed. Three steps in this model are supposed to help the Pd-assisted graphene growth. Firstly, resistive heating makes Pd nanoparticles melt and agglomerate together. Secondly, to go to the second step of the growth model, carbon atoms had to move between Pd nanoparticles, which made graphitic layers around them. Most likely, the process of diffusion happens through both interstitial and vacancy diffusion. The rate of diffusion speeds up when the temperature inside this structure is high. The fact that a graphitic structure forms around Pd shows that it is an active catalyst. Finally, the movement of Pd particles through the whole migration opposite the high resistive area left the graphene structure.

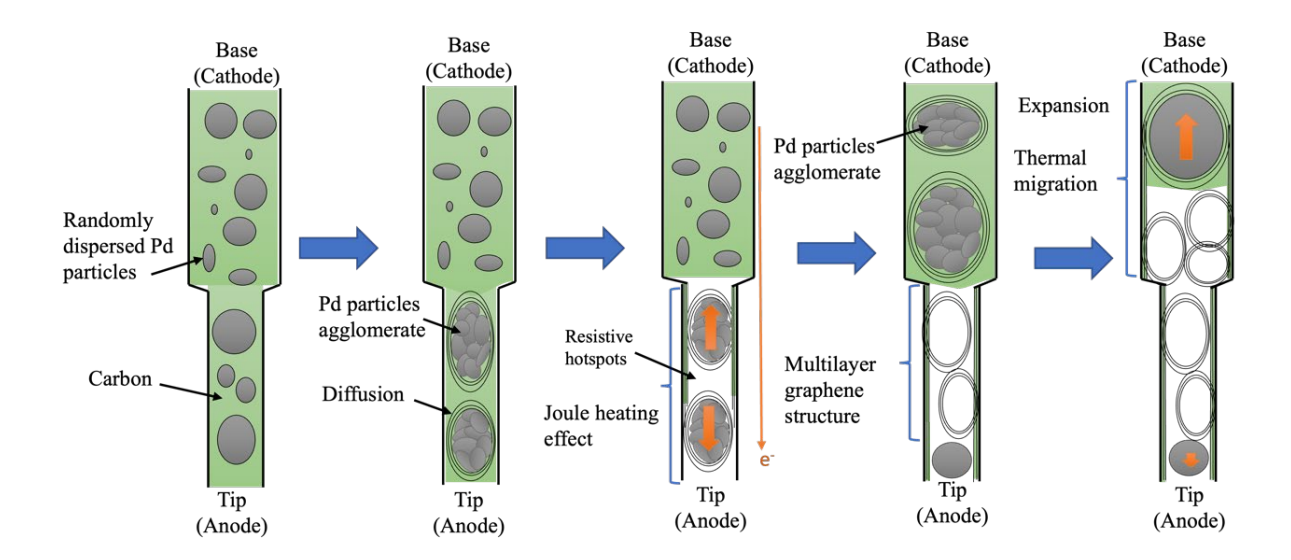


Figure 10: Growth model of Pd-assisted graphene growth

4. CONCLUSIONS

In conclusion, the study has unveiled the solid phase reaction process between Pd and carbon atoms for growing graphene structures using in-situ TEM. This research has provided significant insights into the interaction between Pd and carbon atoms, facilitating the formation of Pd-assisted graphene structures. Notably, the Pd particles undergo recrystallization and agglomeration, moving from the middle part towards the tip and base regions due to the joule heating effect and thermomigration. Concurrently, the amorphous carbon within CNF begins to crystallize, forming sp2 hybridized carbon structures, ultimately resulting in the activation of graphene catalyzed by the presence of Pd particles. The successful synthesis of graphene, spanning approximately 350 nm between the cathode and anode, was achieved within the in-situ TEM environment. This nanoscale observation of graphene formation holds significant implications for comprehending the interaction between carbon atoms and Pd, potentially paving the way for future applications as an electrode for carbon interconnects in integrated circuits.

Acknowledgements

We would like to acknowledge Ministry of Higher Education Malaysia and Universiti Pendidikan Sultan Idris for the research funding (FRGS 2019-0144-103-02). Also, the author would like to thank Nagoya Institute of Technology, Japan for the TEM facility. The first author also would like to thank Universiti Kebangsaan Malaysia for the laboratory facilities and Ministry of Higher Education Malaysia for postdoctoral scholarship award.

Author Contributions

All authors contributed toward data analysis, drafting and critically revising the paper and agree to be accountable for all aspects of the work.

Disclosure of Conflict of Interest

The authors have no disclosures to declare.

Compliance with Ethical Standards

The work is compliant with ethical standard.

References

- [1] Bleu, Y., Bourquard, F., Michalon, J. Y., Lefkir, Y., Reynaud, S., Loir, A. S., Barnier, V., Garrelie, F. & Donnet, C. (2021). Transfer-free Graphene Synthesis by Nickel Catalyst Dewetting using Rapid Thermal Annealing. *Applied Surface Science*, 555, 149492.
- [2] Barth, C. (2018). Carbon Precursor Structures and Graphene on Palladium Nanoparticles. *The Journal of Physical Chemistry C*, 122(1), 522–529.
- [3] Šivec, R., Huš, M., Likozar, B. & Grilc, M. (2022). Furfural Hydrogenation Over Cu, Ni, Pd, Pt, Re, Rh and Ru catalysts: Ab Initio Modelling of Adsorption, Desorption and Reaction Micro-kinetics. *Chemical Engineering Journal*, 436, 135070.
- [4] Easa, J., Jin, R. & O'Brien, C. P. (2020). Evolution of Surface and Bulk Carbon Species Derived from Propylene and Their Influence on the Interaction of Hydrogen with Palladium. *Journal of Membrane Science*, 596, 117738.
- [5] Kwon, S.-Y., Ciobanu, C. V., Petrova, V., Shenoy, V. B., Bareño, J., Gambin, V., Petrov, I. & Kodambaka, S. (2009). Growth of Semiconducting Graphene on Palladium. *Nano Letters*, 9(12), 3985–3990.
- [6]Peng, Z., Somodi, F., Helveg, S., Kisielowski, C., Specht, P. & Bell, A.T. (2012). High-resolution In Situ and Ex Situ TEM Studies on Graphene Formation and Growth on Pt Nanoparticles. *Journal of Catalysis*, 286, 22–29.
- [7] Rosmi, M. S., Yusop, M. Z., Kalita, G., Yaakob, Y., Takahashi, C. & Tanemura, M. (2014). Visualizing Copper Assisted Graphene Growth in Nanoscale. *Scientific Reports*, 4, 7563.
- [8] Hu, Z., Fan, X. & Diao, D. (2023). A Review of In-Situ TEM Studies on the Mechanical and Tribological Behaviors of Carbon-Based Materials. *Lubricants*, 11(5), 187.
- [9] Vicarelli, L., Heerema, S. J., Dekker, C. & Zandbergen, H. W. (2015). Controlling Defects in Graphene for Optimizing the Electrical Properties of Graphene Nanodevices. *ACS Nano*, 9(4), 3428–3435.
- [10] Patera, L. L., Africh, C., Weatherup, R. S., Blume, R., Bhardwaj, S., Castellarin-Cudia, C., Knop-Gericke, A., Schloegl, R., Comelli, G., Hofmann, S. & Cepek, C. (2013). In Situ Observations of the Atomistic Mechanisms of Ni Catalyzed Low Temperature Graphene Growth. *ACS Nano*, 7(9), 7901–7912.

- [11] Eom, H., Joo, H. J., Kim, S. C. & Kim, S. S. (2020). Properties of Carbon-Based Nanofiber with Pd and Its Application to Microbial Fuel Cells Electrode. *Environmental Technology & Innovation*, 19, 100800.
- [12] De Jong, K. P. & Geus, J. W. (2000). Carbon Nanofibers: Catalytic Synthesis and Applications. *Catalysis Reviews*, 42(4), 481–510.
- [13] Sharma, S., Rosmi, M. S., Yaakob, Y., Yusop, M. Z. M., Kalita, G., Kitazawa, M. & Tanemura, M. (2018). In situ TEM Synthesis of Carbon Nanotube Y-junctions by Electromigration Induced Soldering. *Carbon*, 132, 165–171.
- [14] Yaakob, Y., Lin, W. M., Rosmi, M. S., Yusop, M. Z. M., Sharma, S., Chan, K. F., Asaka, T. & Tanemura, M. (2022). Study of Structural and Electrical Behavior of Silicon-Carbon Nanocomposites via In Situ Transmission Electron Microscopy. *Materials Today Communications*, 32, 104081.
- [15] Rosmi, M. S., Yaakob, Y., Yusop, M. Z. M., Sharma, S., Vishwakarma, R., Araby, M. I., Kalita, G. & Tanemura, M. (2016). In Situ Fabrication of Graphene from A Copper–Carbon Nanoneedle and Its Electrical Properties. *RSC Advances*, 6(86), 82459–82466.
- [16] Cui, T., Lv, R., Huang, Z. H., Zhu, H., Jia, Y., Chen, S., Wang, K., Wu, D. & Kang, F. (2012). Low-Temperature Synthesis of Multilayer Graphene/Amorphous Carbon Hybrid Films and Their Potential Application in Solar Cells. *Nanoscale Research Letters*, 7, 453.
- [17] Rosmi, M. S., Yaakob, Y., Yusop, M. Z. M, Isa, I. M., Sidik, S. M., Bakar, S. A. & Masaki, T. (2022). Investigating the Structural Transformation of Individual Au-Incorporated Carbon Nanofiber Interconnect. *Malaysian Journal of Microscopy*, 18(2), 215-224.